

Investigation of metal foam formation by ultra-small angle neutron scattering

J. Banhart

Fraunhofer-Institute for Manufacturing and Advanced Materials, Bremen, Germany

D. Bellmann and H. Clemens

Institute for Materials Research, GKSS Research Centre, Geesthacht, Germany

Zinc foams were prepared by applying the powder compaction method which comprises mixing zinc powder with a small fraction of a blowing agent, compacting this mix and creating a foam by heat treatment above the melting temperature of the metal. The foaming process which normally leads to a volume expansion of some 500% was artificially stopped in very early stages by quenching. The resulting samples which had a porosity below 20% were then characterised by ultra small-angle neutron scattering (USANS). Pore size distributions and total pore volumes were determined. The pore growth behaviour for different size regimes could be obtained from the USANS distribution curves.

1 Introduction

In order to understand how the structure of metal foams is generated it is useful to investigate not only fully expanded foams, but also foams in the early stages of evolution. For this one can apply either in-situ or ex-situ methods. In the former case the evolving foam is monitored during its expansion, e.g. by recording a time-dependent expansion curve [1], or even by generating a picture of the evolving foam using X-ray radiosopic methods [2][3]. In contrast, an ensemble of samples in which each sample represents one particular stage of evolution of the foam is analysed in ex-situ investigations, e.g. by microscopy [1]. The individual samples are prepared by interrupting the foaming process at a given time. If one wants to study the very early stages of foaming, i.e., stages in which the pores are just being formed, one has to apply methods which act on the appropriate length scale which ranges from some tens of nanometers to several micrometers. Optical or electron microscopy, for example, are suitable for investigations if two-dimensional information is sufficient. Often, however, one is less interested in mapping individual pores, but wants to obtain a three-dimensional average of a pore size distribution. Such distributions can be useful, for example, as input data for model calculations of the foam generation process [4]. Ultra small-angle neutron scattering (USANS) is a promising method for obtaining this information because scattering of cold neutrons at very small wave vectors provides exactly the size range required. USANS was therefore chosen for the present study. In order to encounter a fairly simple situation in this study, zinc foams were selected because zinc is known to show a very simple bubble formation pattern when foamed with zirconium hydride, i.e., the bubbles generated are always almost spherical even in the very early stages of foam formation, whereas pore formation in aluminium alloys, for example, is much more complicated [1].

2 Sample preparation

Zinc foam samples were prepared in a three-stage process comprising powder mixing, hot pressing and foaming. First, zinc powder (Eckart-Dorn, type AS; <0.045 mm) was mixed with 0.3 wt.% of zirconium hydride (ZrH_2) powder (Chempur, 99.7% purity) which acted as a blowing agent. For reference measurements, the blowing agent was omitted for one sample. In a second step the powder mix (or the pure metal powder) was filled into a cylindrical die with 32 mm diameter and was pressed at a temperature of 350 °C and a pressure of 110 MPa for 30 minutes. The resulting cylindrical tablets were cut into 4 mm thick slices by electric discharge machining (EDM) and placed onto a support in a furnace pre-heated to 440°C. The sample was quickly warmed up by the pre-heated substrate and remained there for a given

composition of sample	foaming time	density ($g\ cm^{-3}$)	porosity (%)
Zn	0	7.06	0.9
Zn+0.3 wt.% ZrH_2	0	7.05	1.1
	60	7.06	1.0
	70	7.04	1.2
	80	6.98	2.1
Zn+0.3 wt.% ZrH_2	90	6.99	1.9
	100	6.99	1.9
	110	6.94	2.6
	115	6.43	9.8
	120	5.82	18.4

Table 1. Samples prepared for the USANS study.

foaming time t , after which it was removed and immediately quenched to room temperature with pressurised air. A 0.4 mm thick slice was cut out from the centre of the solidified foamed sample by EDM for the USANS measurements. The densities of the thin slices were determined by buoyancy measurement. Table 1 lists all samples examined, including a sample without blowing agent, an unfoamed specimen with blowing agent and 8 different foamed samples.

3 Experimental method

The principal set-up used for USANS studies is shown in Figure 1. A part of the neutron beam coming from the cold source of the reactor is reflected by a pre-monochromator (perfect silicon Si(111) crystal, Bragg-angle 45°) into the double crystal diffractometer (DCD) and then monochromatised using a multi-reflection mirror (quintuple-bounce channel-cut perfect Si(111) crystal with cadmium inserts) [5]. After passing a holding device for changing samples the angle distribution of the neutrons is measured by rotating an analyser crystal (smallest angle steps of 10^{-5} degree) which is identical to the monochromator crystal. The neutrons have a wavelength of $\lambda = 0.443$ nm and a wavelength dispersion of $\Delta\lambda/\lambda \approx 10^{-3}\%$. The average flux at the sample position is about $500\ cm^{-2}\ s^{-1}$. The accessible scattering range is $10^{-5} - 10^{-1}\ nm^{-1}$. Using this technique inhomogeneities (particles, pores, etc.)

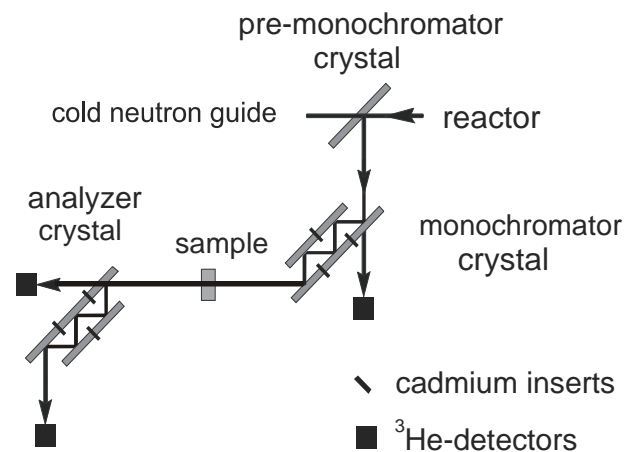


Figure 1. Experimental set-up for USANS measurements using a DCD.

from 24 μm down to 0.03 μm in size are detectable. Deriving the size distribution of pores $v(D)$ from the measured scattering curve $I(q)$ requires some approximations and proper fitting techniques which will be described in a separate paper [6].

4 Results

4.1 Unfoamed samples

The size distributions of scattering centres (differential volume fraction $v(D)$ expressed in volume percent per unit size of pores and/or blowing agent particles) in unfoamed zinc samples as determined by USANS are shown in Figure 2 for specimens with and without blowing agent. The sample without blowing agent shows a maximum in the distribution at diameters of about 1.7 μm . Integration of the distribution curve yields a total volume fraction of scattering centres of 0.17 vol.%. The source for scattering could be residual porosity as well as other metallic impurities which are not accounted for in the data analysis. As residual porosity is certainly not spherical but more fractal in shape, the volume fraction determined

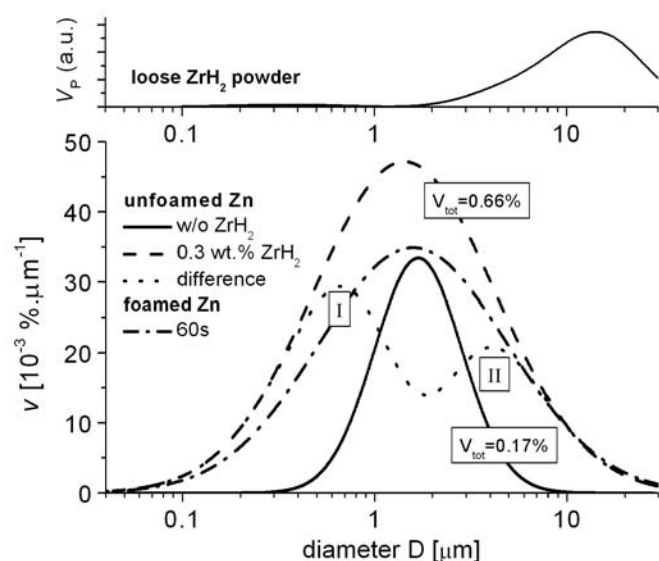


Figure 2. Upper: particle size distribution of loose ZrH_2 powder determined by laser particle analysis. Lower: size distribution $v(D)$ of scattering centres in pressed zinc powder samples with and without ZrH_2 measured by USANS.

should not be thought of as a very accurate value. Indeed, the porosity determined from density measurements ($0.9 \pm 0.3\%$) is higher. The specimen containing ZrH_2 shows a markedly different distribution curve of scattering centres. To demonstrate this, the difference between the two curves was added to Figure 2. It represents the additional features introduced by the hydride powder. Two peaks in the difference distribution curve occur, one for 0.65 μm (peak I), one for 4.2 μm (peak II). The blowing agent is the most obvious source for the additional scattering, but as formation of porosity could be influenced by the presence of ZrH_2 during pressing it should also be considered. One can try to discuss the influence of pores and ZrH_2 separately. This is not possible from the USANS data because we are treating a two-phase system, where the metallic matrix is one phase. However, by making use of the measured particle size distribution of the blowing agent ZrH_2 powder (shown at the top of Figure 2), additional information can be obtained. ZrH_2 particles occur in significant volume fractions above particle diameters of about 2 μm . Particles with 14.7 μm diameter contribute most to the total particle volume while powder particles as large as 60 μm can still be found. As we can only resolve features with diameters up to 24 μm by USANS, the corresponding particle size spectrum is truncated in Figure 2. Noting that the onset of the main particle size distribution peak coincides with the division between the 2 peaks of the USANS difference curve in Figure 2. Therefore it seems reasonable to ascribe most of peak II to the influence of the hydride. Obviously, the powder size distribution, having its maximum at 14.7 μm , does not exactly match the USANS distribution with a maximum at 4.2 μm . This is not surprising if one keeps in mind that the particle size distribution was obtained on loose powders, whereas the USANS curve refers to ZrH_2 powder compacted into a metal matrix. Mixing and subsequent hot compaction will certainly reduce the size and morphology of the brittle hydride powder, therefore leading to a shift of the distribution maximum to lower diameters. Moreover, USANS values for diameters above 24 μm are quite uncertain due to

the limitations mentioned, thus causing an artificial drop-off of the USANS distribution at large diameters. Furthermore, the observed complicated morphology of the ZrH_2 particles deviates from the assumption of spherical particles with a well defined smooth surface which might give rise to an apparent shift in particle size. Peak I may be explained as following: As the size axis in Figure 2 has a logarithmic scale the area under peak I looks quite large although it only accounts for about 8% of the total area under the difference curve (0.49 vol.%). The volume fraction of ZrH_2 is quite small below 1 μm particle size and there is only a very small powder fraction with diameters around 0.4 μm . This, however, is not sufficient to explain peak I. Therefore, most of this peak must arise from some porosity in the specimen in addition to the porosity already present in the sample without blowing agent. One can speculate that the irregularly shaped and brittle particles are not completely embedded in the metal matrix, thus giving rise to additional scattering from satellite voids next to the blowing agent particles. It is also possible that some gas evolution has already started during pressing of the powder mixture. Escaping hydrogen could lead to the formation of small cavities in the solid matrix.

4.2 Foamed samples

Initial foaming stage

Besides the distribution curves for unfoamed precursor material, Figure 2 also includes the USANS distribution curve for the sample with the shortest foaming time, namely 60 seconds, i.e. for the sample which was just approaching its melting temperature and which was about to start foaming. Obviously, the effect of heat treatment is an overall reduction of the volume fraction of scattering centres in this case. The curve remains centred at about 1.5 μm , but the volume fraction is reduced for all diameters. This finding corresponds with a slight increase in sample density (see Table 1) after 60 seconds of heat treatment. Possible reasons for the decrease of the volume fraction of scattering centres: (i) hydrogen losses from ZrH_2 changing the effective scattering length density of the blowing agent. This loss was neglected in our

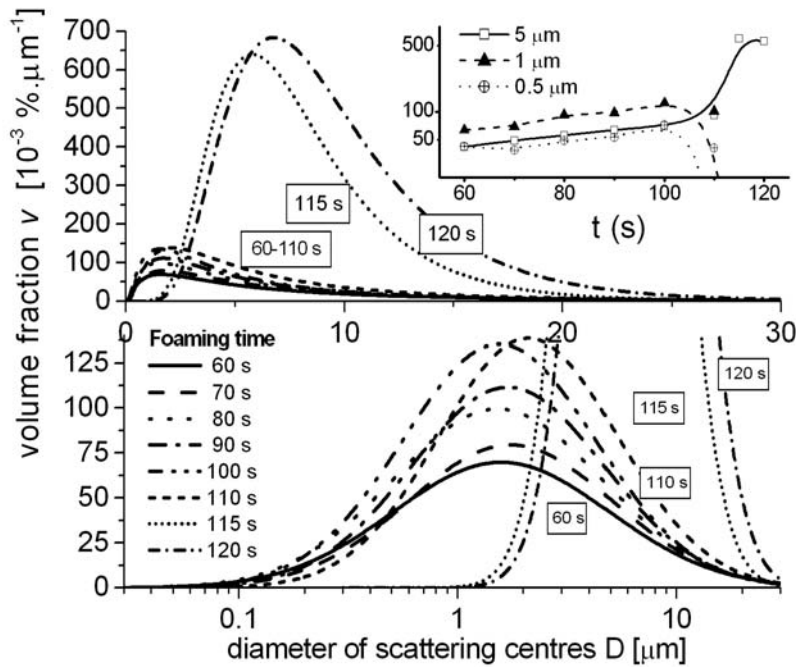


Figure 3. Pore size distributions $v(D)$ in zinc foams. Upper: entire size range with inset showing volume fraction for 0.5, 1 and 5 μm size of scattering centres as a function of time, lower: semi-logarithmic representation restricted to scattering centres with small volume fractions.

analysis and could simulate a decrease of volume, (ii) sintering processes reducing porosity above a certain threshold temperature due to solid-state diffusion processes, (iii) impurities present in the zinc powder forming a liquid phase at temperatures below the melting point which could be absorbed by the residual porosity ("liquid-phase sintering"). As there is evidence for a real volume contraction, the first explanation

can be ruled out and solid or liquid phase sintering processes must be responsible for the observed effect.

Later foaming stages

The volume distribution curves for scattering centres in various zinc foams are shown in Figure 3. The entire information is displayed in the upper part of Figure 3 in a linear plot, whereas the lower part gives insight into the range of small diameters through use of a logarithmic scale and concentrating on the samples with low porosities. Foaming times longer than 60 s lead to an increase in volume fraction of scattering centres on almost all length scales. Obviously, for all times the distribution curves show the log-normal behaviour given by the method of the data analysis. The volume fraction drops to very low values for small diameters and it seems justified to speak of a cut-off diameter. For large diameters the distribution curves are limited by the resolution of the method. The various curves are overlapping and the peak positions are shifted to higher diameters for longer foaming times. The inset in Figure 3 gives volume fractions for some fixed diameters of the scattering centres as a function of foaming time. Obviously, despite of some irregularities for small pore sizes, the curves exhibit a similar pattern: for a given size the volume fraction first rises and then falls down (for 5 μm only the rise can be seen). The physical explanation for this two-stage behaviour is straight-forward: first, small pores are created in large numbers as the sample is heated, presumably by heterogeneous nucleation. Once these pores are present, they grow steadily, driven by gas generation from the blowing agent while no new pores are developed. At the same time they also start to coalesce, thus decreasing the total number of pores and shifting the corresponding contributions of the distribution function to larger diameters. Small pores therefore eventually disappear, thus creating the cut-off diameter while large pores continue to gain importance. Foaming for 120 seconds finally leads to the growth of pores with pore diameters larger than 1 μm with the maximum of the distribution occurring at 7 μm diameter. As it is shown from optical microscopy [6], quite a significant part of the curve now lies in the regime above 24 μm , a size above which the USANS is not reliable. Therefore, it makes no sense to investigate the further foam evolution with this DCD configuration. However, by decreasing the neutron wavelength of DCD using perfect Si(311) crystals larger structures could be detectable in future experiments.

4.3 Total (integrated) volume fraction

What becomes clear at this point is that pore inflation starts rather suddenly after a longer stage of gradual expansion and then proceeds very quickly. The macroscopic density shows the same behaviour (Table 1). From the unfoamed sample to the sample foamed up to 110 s the density decreases by just 1.5%, whereas the following 10 seconds of heat treatment result in an expansion of 17%. Similar results can be obtained from the USANS measurements by calculating the total pore volume V'_{tot} by integration over the distribution function $v(D,t)$:

$$V'_{tot}(t) = \int_0^{D_{\max}} v(D,t) dD < V_{tot}(t)$$

The total volume fraction has been primed to emphasise that only the fraction of scattering centres accessible to USANS is included in it (D_{\max} is 24 μm in our case). Figure 4 compares the total volume fractions determined in this way with conventionally measured relative sample densities, i.e. ρ/ρ_0 , where ρ_0 is the bulk density. Obviously, the functional dependence of both quantities is very similar, but the total volume fractions determined by USANS are only about half as large. The two regimes which were already discussed in the previous section are clearly visible: in region I the volume slightly decreases, in region II there is a steady volume increase which is almost linear with time as shown by the linear fit curve. In

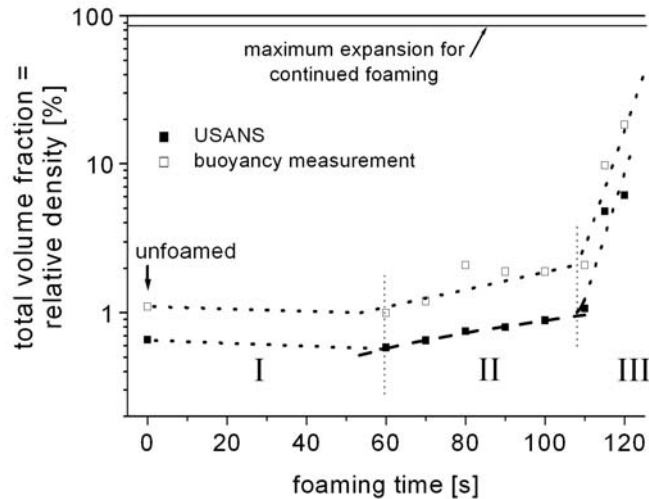


Figure 4. Total volume fraction V'_{tot} of pores in foamed zinc as a function of foaming time at 350 °C determined by buoyancy measurement and USANS. The dotted lines are merely for orientation, whereas the dashed line represents a linear fit.

region III, however, rapid pore formation starts which eventually leads to a fully expanded foam with 85% porosity. Possible reasons for the discrepancy between the two measurements were also addressed in the previous section: (i) deviations of pore morphology from the spherical shape and, (ii) the inability of this DCD to detect inhomogeneities greater than round about 24 μm in size. While the first explanation might apply to early foams, the second is definitely applicable to the more expanded foams, as they contain many very large pores.

4 Summary

Zinc foams were produced by expanding powder compacts containing Zn powder and zirconium hydride which acted as a blowing agent. By varying the time of heat treatment and quenching the emerging foams after this time, different stages of early foam formation could be prepared. It has been found that by adding ZrH_2 to Zn powders the porosity of the compacted powders is increased. Either by mechanical action or by gas release during compaction porosity is created on a sub-micrometer scale. Foaming of powder compacts containing ZrH_2 first leads to a decrease of this sub- μm porosity resulting from either solid-state diffusion processes or liquid-phase sintering. After this a steady creation of porosity in all size ranges is observed. The maximum of the pore size distribution moves to larger diameters while smaller pores disappear. The foaming process is quite slow for a long period, thereafter bubble inflation starts suddenly. In this phase of accelerated bubble growth, a large pore volume is generated with a maximum pore diameter at 7.5 μm for the most mature foam investigated and, additionally, many bubbles exceed the maximum size measurable by USANS.

References

- [1] Duarte I., Banhart J., *Acta Mater.* **48**, 2349 (2000)
- [2] Banhart J., Stanzick H., Helfen L., Baumbach T., *Appl. Phys. Lett.* **78**, 1152 (2001)
- [3] Banhart J., Stanzick H., Helfen L., Baumbach T., *Adv. Eng. Mat.* **3**, 407 (2001)
- [4] Körner C., Singer R.F., in „Metal Foams and Porous Metal Structures“, Ed. J. Banhart, M.F. Ashby, N.A. Fleck, MIT-Verlag, Bremen (2001), p. 91
- [5] Bellmann D., Staron P., Becker P., *Physica B* **276-278**, 124 (2000)
- [6] Banhart J., Bellmann D., Clemens H., *Acta Mater.* **49**, 3409 (2001)